Forward and inverse kinematics of a hybrid series-parallel manipulator

Sachit Rao, Jagannath Raju

Abstract

In this paper, the forward and inverse kinematic relations of a hybrid 6-DOF robotic manipulator, named the H6AR, are presented. The H6AR consists of twin 2-DOF anthropomorphic arms that can move in the vertical plane. These arms are connected, at one end, to a 1-DOF waist and constrained, at the other end, by a novel wrist assembly. The wrist contains an actuator only for the pitching motion and due to its unique design, by moving only the twin arms, the yaw and roll motions are generated. Closed-form forward and inverse kinematic relations are presented by following the Denavit-Hartenberg technique.

Keywords: Hybrid Manipulator, Kinematics, Closed-form solutions

1 Introduction

In this paper, the forward and inverse kinematic relations of a hybrid 6 degree-of-freedom (DOF) manipulator, named the Hybrid 6-Axis Articulated Robot (H6AR)*, are presented. The H6AR offers the attractive properties of large achievable workspaces and higher payload carrying capacities that are possessed by conventional serial and parallel manipulators, respectively. Conventional serial link manipulators, that are easy to control and have a large achievable workspace, require the placement of actuators at locations that limit their payload carrying capacities and make them heavy. Although light-weight materials have been used to construct them, issues related to the flexibility of such materials arise, [3]. On the other hand, parallel manipulators, such as the Stewart platform [2], have their actuators near the base and are able to carry large payloads. But, these manipulators have a much limited workspace and often require computationally expensive solutions for their control. Indeed, solutions that attempt to combine both these designs have been offered. The idea of using several anthropomorphic arms that cooperate with each other in performing a task is demonstrated in [1] and [5]. Other series-parallel hybrid designs are presented in [4] and [8]. A variant of the serial link manipulator, in which the actuators are located close to the base, is the "dual-elbow" manipulator, [9].

The H6AR consists of a waist to which twin anthropomorphic arms that are separated by a fixed distance are connected. These arms are passively connected to a unique compact wrist assembly that contains a single actuator used to generate the pitching motion. The yaw and roll motions are generated by only moving the twin arms and

Sachit Rao (Corresponding author)
Systemantics India Pvt Ltd, Bangalore, India, E-mail: sachit@systemantics.com

Jagannath Raju
Systemantics India Pvt Ltd, Bangalore, India, E-mail: gjraju@systemantics.com

*Indian and US patents are pending

hence, the actuators for these 2 DOFs are completely eliminated. The 4 actuators that drive the joints of the twin arms are located close to the waist.

The paper is organised as follows: In Sec. 2, the construction of the H6AR and its parameters are described. In Sec. 3, using the Denavit-Hartenberg (D-H) technique, the forward kinematic relations that yield the coordinates of the wrist-tip are derived. Finally, in Sec. 4, the inverse kinematic relations, which yield the joint angles when the tip coordinates and the orientation angles are known, are presented.

2 Description of the H6AR

In this section, a basic description of the components of the H6AR is provided. The schematic of the robot and its wrist are shown in Fig. 1.

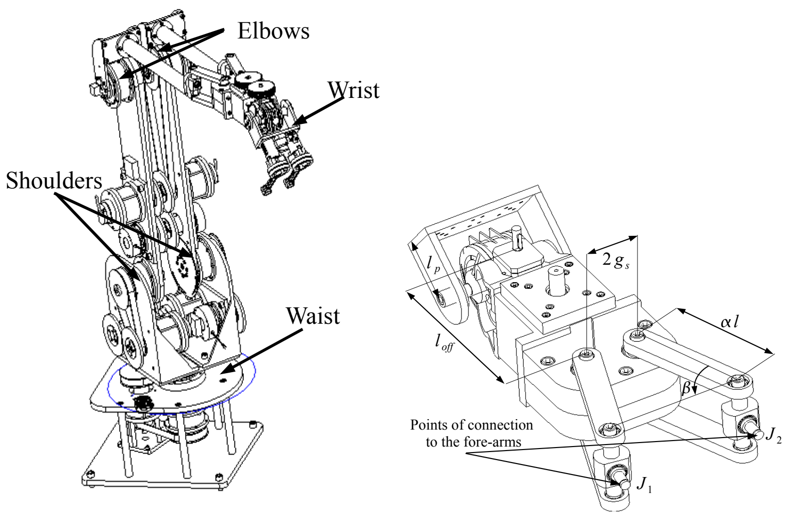

(a) (b)

Figure 1: Schematics of: (a) the H6AR and (b) the H6AR wrist

The entire H6AR assembly is mounted on a stationary base. The waist of the robot, which rotates in the horizontal plane, is mounted at the centre of the base. Also, the twin anthropomorphic arms, which rotate in the vertical plane, are connected to the waist at a fixed distance, termed as the mid-plane offset, from the waist centre. Each of these arms is comprised of two links, denoted as the upper-arm and the fore-arm. Further, these arms are connected through passive 2-DOF joints, denoted by J_1 and J_2, to the wrist assembly. The wrist assembly, whose schematic is shown in Fig. 1(b), resembles the well-known 4-bar linkage system, but consists of a spur gearset, which replaces one of the bars. With such a design, yaw and roll motions are generated by moving only the shoulder and elbow joints. The gearset also ensures that the wrist assembly remains symmetric during the yaw and roll motions. These motions are generated by moving the tips of the fore-arms reflective-symmetrically about a point that lies in the mid-plane of the two arms and on a line normal to this plane and connecting the tips of the fore-arms when the roll and yaw angles are zero. This point is termed as the "invariant" point. The wrist assembly also consists of a link to which the tool/gripper is attached that is driven by a separate actuator to generate the pitching motion.

The physical parameters of the H6AR are as follows. Each of the upper-arms and the fore-arms has a length of L_1 and L_2, respectively. The mid-plane offset has a length d. As shown in Fig. 1(b), the wrist parameters are given by the distances $\alpha l, 2g_s$, and l_{off} and the angle β, termed as the separation angle. αl and $2g_s$ denote the lengths of the links and the distance between the gears, respectively, while l_{off} is the length of the link that connects the wrist to the pitch joint. The link that undergoes the pitching motion, to which the payload is attached, has a length l_p. The parameters αl and β are designed so that the wrist does not assume a singular configuration for the allowed roll and yaw angles. The procedure to design them is presented in Sec. 3.4.

The joint angles of H6AR are denoted as follows: the waist joint angle by θ_1; the shoulder joints by θ_2^L and θ_2^R, where θ_2^L is the left shoulder angle when the H6AR is viewed with the fore-arms going into the paper; the elbow joint angles are similarly labeled as θ_3^L and θ_3^R. The yaw, roll, and pitch angles are denoted by ψ, ϕ, and θ, respectively.

To show that the H6AR does have 6 DOFs, Grübler's formula applicable for mechanisms with loops [6], given by the general expression $M = \sum_{i=1}^{p} f_i - 6l$, where l is the number of independent kinematic loops, is used. In this equation, M is the total number of DOFs, p denotes the number of joints, and f_i is the DOF of the i^{th} joint. The H6AR mechanism contains one independent kinematic loop, hence $l = 1$ and from the joints' names and their DOFs, listed in Table 1, it can be seen that $M = 6$.

Name	DOF (f_i)
Waist	1
Twin shoulders	2
Twin elbows	2
Joints J_1 and J_2	4
Wrist joints (gearset)	2
Pitch	1
Total	$\sum_{i=1}^{p} f_i = 12$

Table 1: Joints of the H6AR and their DOFs

Note that the same result can be derived by the use of Kutzbach's criterion for spatial mechanisms. By representing the wrist mechanism in terms of links connected only by single DOF revolute joints, it can be shown that, by applying Kutzbach's criterion, $M = 6$.

3 Forward Kinematics

In this section, the forward kinematic relations that yield the tip coordinates are derived using the D-H technique described in [7]. First, the coordinates of the tips of the fore-arms are calculated in terms of the waist, shoulders', and elbows' joint angles. Next, an equivalent serial mechanism that lies in the mid-plane of the twin arms is constructed such that the tip of this mechanism is the invariant point and finally, the tip coordinates are calculated with respect to this point.

3.1 Tips of the fore-arms

The coordinate frames and D-H parameters of the waist, right shoulder, and right elbow joints of the H6AR are assigned as shown in Fig. 2. The parameter a_1 is set to zero. The mid-plane offset, d, is related to these parameters by the equation $d = d_2 + d_3$. The Y-axis of each of these coordinates frames, not shown in Fig. 2, is chosen to complete a right-hand system. A similar procedure is followed for the left-side components as well. All counter-clockwise rotations are considered to be positive. By denoting the

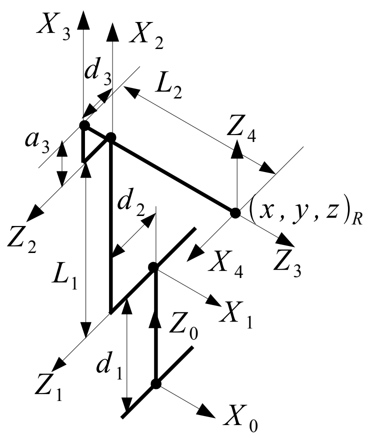

i	a_i	d_i	α_i	θ_i
1	a_1	d_1	$\frac{\pi}{2}$	θ_1
2^R	L_1	d_2	0	θ_2^R
3^R	a_3	d_3	$\frac{\pi}{2}$	θ_3^R
4^R	0	L_2	$\frac{\pi}{2}$	θ_4^R

Figure 2: Coordinate frames and D-H parameters of the waist and the twin shoulder and elbow joints

coordinates of the tips of the left and right fore-arms as $(x, y, z)_R$ and $(x, y, z)_L$, their values are given by

$$x_R = s_1 d + c_1 \left(L_1 c_2^R + L_2 s_{23}^R + a_3 c_{23}^R\right), \ (c)s_i = (\cos)\sin\theta_i \quad \text{(1a)}$$
$$y_R = -c_1 d + s_1 \left(L_1 c_2^R + L_2 s_{23}^R + a_3 c_{23}^R\right) \quad \text{(1b)}$$
$$z_R = d_1 + L_1 s_2^R - L_2 c_{23}^R + a_3 s_{23}^R, \ (c)s_{ij} = (\cos)\sin(\theta_i + \theta_j) \quad \text{(1c)}$$

and

$$x_L = -s_1 d + c_1 \left(L_1 c_2^L + L_2 s_{23}^L + a_3 c_{23}^L \right) \tag{2a}$$
$$y_L = c_1 d + s_1 \left(L_1 c_2^L + L_2 s_{23}^L + a_3 c_{23}^L \right) \tag{2b}$$
$$z_L = d_1 + L_1 s_2^L - L_2 c_{23}^L + a_3 s_{23}^L, \tag{2c}$$

respectively. In the next section, these coordinates are used to derive those of the invariant point.

3.2 Invariant point–forward kinematics

As mentioned before, the roll and yaw motions are generated by moving the twin arms reflective-symmetrically about the invariant point. Such motions are selected so that unique shoulders' and elbows' joint angles can be found that yield the given yaw and roll angles.

The reflective-symmetric motions and the location of the invariant point, whose coordinates are denoted by $(x, y, z)_I$, can be identified from Fig. 3, which shows the projections of the wrist on the $(X, Y)_0$ and $(Y, Z)_0$ planes. Fig. 3(a) shows the projection when the robot is performing a pure yawing motion for some $\theta_1, \theta \neq 0$. Since the rolling motion is indepedent of the waist angle, Fig. 3(b) shows the projection for a pure rolling motion for $\theta_1 = 0$ and $\theta \neq 0$. Note that the pitching motion is provided by a separate actuator located at the wrist. Due to the reflective-symmetric motion that

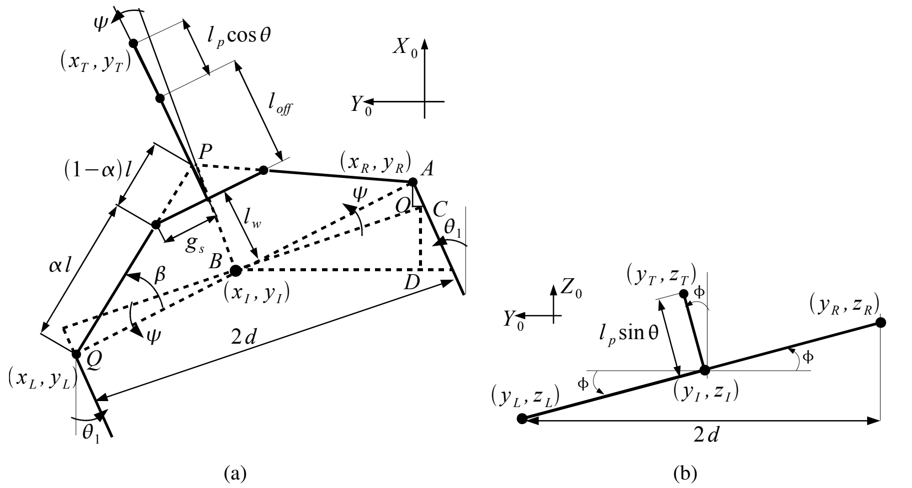

Figure 3: Projections of the H6AR wrist on the (a) $(X, Y)_0$ plane and on the (b) $(Y, Z)_0$ plane

generates the roll angle, from Fig. 3(b), the coordinate z_I is given by

$$z_I = z_R - d \tan\phi, \ z_I = z_L + d \tan\phi. \tag{3}$$

Similarly, to calculate the coordinates $(x, y)_I$, consider Fig. 3(a). From the triangles ΔAOC and ΔBCD, it can be shown that

$$x_I = x_R - d\,(\tan\psi\cos\theta_1 + \sin\theta_1) \tag{4a}$$
$$y_I = y_R + d\,(\cos\theta_1 - \tan\psi\sin\theta_1)\,. \tag{4b}$$

Since the left-hand part of the wrist assembly is symmetric, the relations

$$x_I = x_L + d\,(\tan\psi\cos\theta_1 + \sin\theta_1) \tag{5a}$$
$$y_I = y_L - d\,(\cos\theta_1 - \tan\psi\sin\theta_1) \tag{5b}$$

can be derived. Thus, these relations lead to the simple results

$$x_I = \frac{x_R + x_L}{2},\ y_I = \frac{y_R + y_L}{2},\ z_I = \frac{z_R + z_L}{2}. \tag{6}$$

From (1) and (2) and the fact that the point $(x, y, z)_I$ is invariant to the reflective-symmetric motions, its coordinates when expressed in terms of the joint angles are given by

$$x_I = c_1\left[L_1 c_2^A + L_2 s_{23}^A + a_3 c_{23}^A\right], \tag{7a}$$
$$y_I = s_1\left[L_1 c_2^A + L_2 s_{23}^A + a_3 c_{23}^A\right], \tag{7b}$$
$$z_I = d_1 + L_1 s_2^A - L_2 c_{23}^A + a_3 s_{23}^A,\ \theta_i^A = \frac{\theta_i^R + \theta_i^L}{2},\ i = 2, 3. \tag{7c}$$

3.3 Equivalent serial mechanism

Comparing the coordinates of the invariant point, given by (7), and those of the tips of the fore-arms, given by (1) and (2), an equivalent serial mechanism lying in the mid-plane of the actual twin arms and whose fore-arm tip has the coordinates $(x, y, z)_I$ can be constructed. From (7), it is clear that the link lengths of this virtual mechanism are L_1 and L_2 and that its joint angles are the averages of the respective actual joint angles. In addition, from Fig. 3(a), the wrist assembly that undergoes the roll and yaw can be reduced to an equivalent single link of length $L_W = (l_W + l_{\text{off}})$ where, using simple geometric relations, it can be shown that the length l_W is dependent on the yaw angle and is given by

$$l_W = \sqrt{(\alpha l)^2 - \frac{(\alpha d)^2}{\cos^2\psi}},\ \alpha = 1 - \frac{g_s\cos(\psi)}{d}. \tag{8}$$

3.4 Wrist

To determine the coordinates of the tip, denoted by $(x, y, z)_T$, the coordinate frames and the D-H parameters are assigned to the wrist as shown in Fig. 4. Note that the frames $(X, Y, Z)_{3V}$ and $(X, Y, Z)_{4V}$ have the same orientation as the frames $(X, Y, Z)_3$ and $(X, Y, Z)_4$ as shown in Fig. 2. Following the procedure used to de-

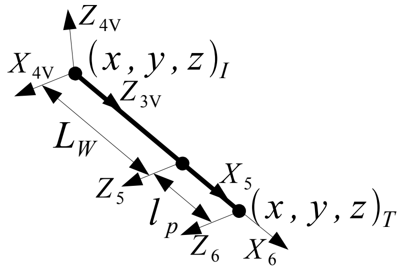

i	a_i	d_i	α_i	θ_i
4	0	L_2	$\frac{\pi}{2}$	$\frac{\pi}{2}+\phi$
5	L_W	0	$\frac{\pi}{2}$	$\frac{\pi}{2}+\psi$
6	l_p	0	0	θ

Figure 4: Coordinate frames and D-H parameters of the wrist

termine the coordinates of the tips of the fore-arms, the tip coordinates are given by

$$x_T = c_1\left(L_1 c_2^A + L_{2W} s_{23}^A + a_{3W} c_{23}^A\right) - s_1 L_\theta \tag{9a}$$

$$y_T = s_1\left(L_1 c_2^A + L_{2W} s_{23}^A + a_{3W} c_{23}^A\right) + c_1 L_\theta \tag{9b}$$

$$z_T = d_1 + L_1 s_2^A - L_{2W} c_{23}^A + a_{3W} s_{23}^A \tag{9c}$$

$$L_\theta = (L_W + l_p c_\theta)\, c_\phi s_\psi - l_p s_\theta s_\phi,$$

$$L_{2W} = L_2 + (L_W + l_p c_\theta)\, c_\psi,\ a_{3W} = a_3 + (L_W + l_p c_\theta)\, s_\phi s_\psi + l_p s_\theta c_\phi.$$

The yaw and roll angle ranges, denoted by $|\psi| \le \psi_{\max}$ and $|\phi| \le \phi_{\max} = \psi_{\max}$, are decided by the mid-plane offset, the wrist link length αl, and the separation angle β. Note that no angular constraints are imposed on the passive joints J_1 and J_2. But, the wrist can assume a singular configuration for certain values of ψ within the chosen range if the wrist parameters are not properly designed. In order that this singularity does not result, β is chosen such that $\beta = \beta_{\min} > 0°$ when $|\psi| = \psi_{\max}$. Now, to design the length αl, consider the triangle ΔPQB in Fig. 3(a). Based on this constraint on β and the expression for the ratio α, given by (8), it can be shown that if the wrist link length is selected to satisfy

$$\alpha l \ge \frac{d - g_s \cos(\psi_{\max})}{\cos(\psi_{\max})\cos(\beta_{\min})}, \tag{10}$$

then, the wrist does not assume the singular configuration. This result also holds for any roll angle $|\phi| \le \phi_{\max}$.

4 Inverse Kinematics

In this section, the joint angles of the twin shoulder and elbow joints and that of the waist are derived when the tip coordinates and the orientation angles are given. First, the waist angle is determined. Next, the coordinates of the invariant point and those of the tips of the forearms are calculated, which are then used to determine the shoulder and elbow joints' angles.

Waist Angle: From (9a) and (9b), the relation

$$-s_1 x_T + c_1 y_T = L_\theta \tag{11}$$

can be derived. To solve this transcendental equation, the identity

$$\frac{\kappa \sin x + \rho \cos x}{\sqrt{\kappa^2 + \rho^2}} = \sin(x + \gamma)\,,\ \gamma = \begin{cases} \sin^{-1}\left(\dfrac{\rho}{\sqrt{\kappa^2+\rho^2}}\right) & \text{if } \kappa \geq 0, \\ \pi - \sin^{-1}\left(\dfrac{\rho}{\sqrt{\kappa^2+\rho^2}}\right) & \text{if } \kappa < 0, \end{cases} \tag{12}$$

is used. Applying this identity to (11) leads to the waist angle being given by

$$\theta_1 = \sin^{-1}\left(\frac{L_\theta}{\sqrt{x_T^2 + y_T^2}}\right) - \gamma_1,\ \gamma_1 = \begin{cases} \sin^{-1}\left(\dfrac{y_T}{\sqrt{x_T^2+y_T^2}}\right) & \text{if } x_T < 0, \\ \pi - \sin^{-1}\left(\dfrac{y_T}{\sqrt{x_T^2+y_T^2}}\right) & \text{if } x_T \geq 0, \end{cases}.$$

Invariant Point: To evaluate the coordinates $(x, y, z)_I$ given by (7), the angles θ_2^A and θ_3^A need to be determined. The angle θ_3^A is evaluated using the relation

$$2L_1\left(L_{2W} s_3^A + a_{3W} c_3^A\right) = (c_1 x_T + s_1 y_T)^2 + (z_T - d_1)^2 - L_1^2 - L_{2W}^2 - a_{3W}^2 = L_{3A},$$

which is derived using (9). Again applying the identity (12), it can be shown that

$$\theta_3^A = \sin^{-1}\left(\frac{L_{3A}}{2L_1\sqrt{L_{2W}^2 + a_{3W}^2}}\right) - \sin^{-1}\left(\frac{a_{3W}}{\sqrt{L_{2W}^2 + a_{3W}^2}}\right) \tag{13}$$

for $|\theta, \psi| \leq 90°$. Next, by solving the simultaneous equations

$$\begin{aligned} (c_1 x_T + s_1 y_T)\, c_{23}^A + (z_T - d_1)\, s_{23}^A &= L_1 c_3^A + a_{3W} \\ (c_1 x_T + s_1 y_T)\, s_{23}^A - (z_T - d_1)\, c_{23}^A &= L_1 s_3^A - L_{2W}, \end{aligned}$$

the angle θ_2^A can be obtained from the sum

$$\theta_{23}^A = \tan^{-1}\left(\frac{(z_T - d_1)\left(L_1 c_3^A + a_{3W}\right) + (c_1 x_T + s_1 y_T)\left(L_1 s_3^A + L_{2W}\right)}{(c_1 x_T + s_1 y_T)\left(L_1 c_3^A + a_{3W}\right) - (z_T - d_1)\left(L_1 s_3^A + L_{2W}\right)}\right). \tag{14}$$

Twin Shoulder and Elbow Angles: Since the average of the twin shoulder and elbow angles, θ_2^A and θ_3^A, respectively, are known, it is sufficient to find only one set of angles, say θ_2^R, θ_3^R (or θ_2^L, θ_3^L). In addition, if $\psi = \phi = 0$, then $\theta_2^R = \theta_2^L = \theta_2^A$ and $\theta_3^R = \theta_3^L = \theta_3^A$. Here, only the calculation of θ_2^R and θ_3^R is illustrated.

Since the coordinates $(x, y, z)_I$ are known, the coordinates $(x, y, z)_R$ are calculated using the relations (3) and (4). Thus, similar to the calculation of θ_3^A, using (1), θ_3^R is given by

$$\theta_3^R = \sin^{-1}\left(\frac{(c_1 x_R + s_1 y_R)^2 + (z_R - d_1)^2 - L_1^2 - L_2^2 - a_3^2}{2L_1\sqrt{L_2^2 + a_3^2}}\right) - \sin^{-1}\left(\frac{a_3}{\sqrt{L_2^2 + a_3^2}}\right).$$

The angle θ_2^R is calculated by following the procedure used to evaluate θ_2^A and is given by

$$\theta_{23}^R = \tan^{-1}\left(\frac{(z_R - d_1)\left(L_1 c_3^R + a_3\right) + (c_1 x_R + s_1 y_R)\left(L_1 s_3^R + L_2\right)}{(c_1 x_R + s_1 y_R)\left(L_1 c_3^R + a_3\right) - (z_R - d_1)\left(L_1 s_3^R + L_2\right)}\right).$$

5 Conclusions

The unique design of the H6AR mechanism offers the robot a combination of the desirable properties of serial and parallel manipulators. As shown in this paper, the closed-form forward and inverse kinematic relations are computationally inexpensive, which in turn implies that the H6AR can be easily controlled.

References

[1] T . Arai, K . Yuasa, Y . Mae, K . Inoue, K . Miyawaki, and N . Koyachi. A hybrid drive parallel arm for heavy material handling. *IEEE Robotics & Automation Magazine*, 9(1):45–54, 2002.

[2] B . Dasgupta and T . S . Mruthyunjaya. The Stewart platform manipulator: a review. *Mechanism and Machine Theory*, 35:15–40, 2000.

[3] S . K . Dwivedy and P . Eberhard. Dynamic analysis of flexible manipulators, a literature review. *Mechanism and Machine Theory*, 41:749–777, 2006.

[4] J . F . Gardner, V . Kumar, and J . H . Ho. Kinematics and control of redundantly actuated closed chains. In *Proceedings of the IEEE International Conference on Robotics and Automation, 1989*, volume 1, pages 418–424, May 1989.

[5] D . Kanaan, P . Wenger, and D . Chablat. Kinematic analysis of a serial-parallel machine tool: The VERNE machine. *Mechanism and Machine Theory*, 44:487–498, 2009.

[6] M . Shoham and B . Roth. Connectivity in open and closed loop robotic mechanisms. *Mechanism and Machine Theory*, 32(3):279–293, 1997.

[7] M . W . Spong, S . Hutchinson, and M . Vidyasagar. *Robot Dynamics and Control*. Second edition, January 2004.

[8] T . K . Tanev. Kinematics of a hybrid (parallel–serial) robot manipulator. *Mechanism and Machine Theory*, 35:1183–1196, 2000.

[9] V . D . Tourassis and D . M . Emiris. A comparative study of ideal elbow and dual-elbow robot manipulators. *Mechanism and Machine Theory*, 28(3):357–373, 1993.